Comparison of the Energy-Band Structure of Ge-Si with Those of Si and Ge

D. J. Stukel
Aerospace Research Laboratories, Wright-Patterson Air Force Base, Ohio 45433
(Received 8 October 1970)

A first-principles self-consistent orthogonalized-plane-wave energy-band calculation has been performed for Ge-Si using a nonrelativistic formalism and Slater's free-electron exchange approximation. The imaginary part of the dielectric constant, valence- and conduction-band densities of states, spin-orbit splittings, deformation energies, and the x-ray form factors (Fourier transforms of the electron charge density) have been calculated and compared with the results obtained for Si and Ge. The theoretical results are compared with experimental data.

I. INTRODUCTION

The group-IV semiconductors Si and Ge have been studied extensively, both experimentally and theoretically. One method which has been used to obtain information on the band structure of these simple semiconductors has been to study the change produced in their physical properties by alloying one semiconductor with another.

In this work a self-consistent calculation has been performed for Ge-Si. In the "virtual-crystal" approximation, Ge-Si corresponds to the alloy $Ge_{0.5}Si_{0.5}$. This work was motivated by an interest in seeing how the band structure and related optical properties of Ge-Si compare with those of Ge and Si. It is also of interest to see how the results of the perfect-lattice Ge-Si calculation agree with the experimental results found for the $Ge_{0.5}Si_{0.5}$ alloy.

The purpose of this work is to compare the Si, Ge-Si, and Ge band structures and related optical properties. These optical properties include the effect of pressure on the band structure, spin-orbit splittings, deformation energies, valence- and conduction-band densities of states, imaginary part of the dielectric constant ϵ_2, and the x-ray form factors (the Fourier transform of the electron charge density). These calculations were performed using the self-consistent orthogonalized-plane-wave (SCOPW) model developed at the Aerospace Research Laboratories (ARL). These self-consistent-model programs have been very successful in calculating the energy-band structures of group III-V,[1-5] II-VI,[6-8] and IV[9] compounds.

In Sec. II calculational details of the model are discussed. The SCOPW results are given, discussed, and compared with each other and with experimental results in Sec. III. Conclusions are presented in Sec. IV.

II. CALCULATIONAL DETAILS

SCOPW Calculations

The OPW method of Herring[10] is used to calculate the electron energies. In the SCOPW model,[6,7,11] the electronic states of the crystal are divided into tightly bound core states and loosely bound valence states which are handled quite differently. The following two assumptions are made about these states: (a) The core states at different atom sites do not overlap. (b) The potential seen by the core states can be considered spherically symmetric.

The valence states must be well described by a modified Fourier series

$$\psi_{k_0}(r) = \sum_\mu B_\mu \left[\Omega_0^{-1/2} e^{i\vec{k}_\mu \cdot \vec{r}} - \sum_a e^{i\vec{k}_\mu \cdot \vec{R}_a} \sum A^a_{c\mu} \psi_c(r - R_a)\right],$$

where $k_\mu = k_0 + K_\mu$, k_0 locates the electron within the first Brillouin zone, K_μ is a reciprocal-lattice vector, R_a is an atom location, ψ_c is a core wave function, and Ω_0 is the volume of the crystalline unit cell. The coefficients $A^a_{c\mu}$ are determined by requiring that $\psi_{k_0}(r)$ be orthogonal to all core-state

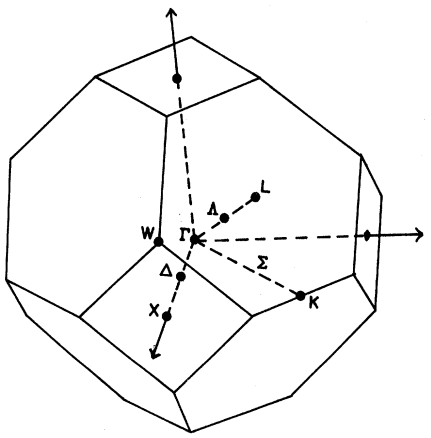

FIG. 1. Zinc-blende Brillouin zone with high-symmetry points labeled. Δ and Σ are symmetries possessed by the Γ-X and Γ-K lines. In our calculations the midpoints of the lines were used for the Δ point $(\frac{1}{2}, \frac{1}{2}, 0)$ and Σ point $(\frac{1}{2}, \frac{1}{2}, 0)$.

TABLE I. Non-self-consistent eigenvalues obtained using different numbers of OPW's at the Γ point are given for Si, Ge-Si, and Ge. All entries are in eV.

	Si				Ge-Si				Ge			
Number of OPW's	Γ_1	$\Gamma_{25'}$	$\Gamma_{2'}$	Γ_{15}	Γ_1	$\Gamma_{25'}$	$\Gamma_{2'}$	Γ_{15}	Γ_1	$\Gamma_{25'}$	$\Gamma_{2'}$	Γ_{15}
27	−55.81	−42.73	−41.14	−39.92	−54.16	−40.89	−40.39	−38.11	−52.31	−38.89	−39.62	−36.15
89	−55.84	−43.96	−41.25	−40.77	−54.20	−42.10	−40.56	−38.91	−52.38	−40.10	−39.89	−36.91
137	−55.84	−44.19	−41.27	−40.88	−54.20	−42.31	−40.57	−39.01	−52.38	−40.29	−39.89	−36.99
181	−55.85	−44.23	−41.28	−40.92	−54.21	−42.35	−40.58	−39.04	−52.38	−40.32	−39.90	−37.01
259	−55.85	−44.26	−41.30	−40.94	−54.21	−42.37	−40.60	−39.06	−52.39	−40.34	−39.91	−37.02
387	−55.85	−44.28	−41.30	−40.97	−54.21	−42.38	−40.60	−39.07	−52.39	−40.34	−39.91	−37.03

wave functions. The variation of B_μ to minimize the energy then results in the valence one-electron energies and wave functions.

The division of the electronic states of the crystal into core and valence states is governed primarily by the requirements that the core wave functions at different atom sites do not overlap and that the valence wave-function OPW Fourier expansion converges within a reasonable number of OPW's. The $3s$ and $3p$ states of Si and $4s$ and $4p$ states of Ge are taken as the valence states.

The calculation is self-consistent in the sense that the core and valence wave functions are calculated alternately until neither changes appreciably. The Coulomb potential due to the valence electrons and the valence charge density are both spherically symmetrized about each inequivalent atom site. With these valence quantities frozen, new core wave functions are calculated and iterated until the core functions are mutually self-consistent. The total electronic charge density is calculated at 650 crystalline mesh points covering $\frac{1}{24}$ of the unit cell, and the Fourier transform of $\rho(r)^{1/3}$ is calculated. The new crystal potential is calculated from the old valence charge distribution and the new core charge distribution. Then new core-valence orthogonality coefficients $A^a_{c\mu}$ are calculated. The iteration cycle is completed by the calculation of new valence energies and wave functions. The iteration process is continued until the valence one-electron energies change less than 0.01 eV from iteration to iteration.

The appropriate charge density to use for both the self-consistent potential calculation and the form-factor calculation is the average charge density of all the electrons in the Brillouin zone. In the present self-consistent calculations this average is approximated by a weighted average over elec-

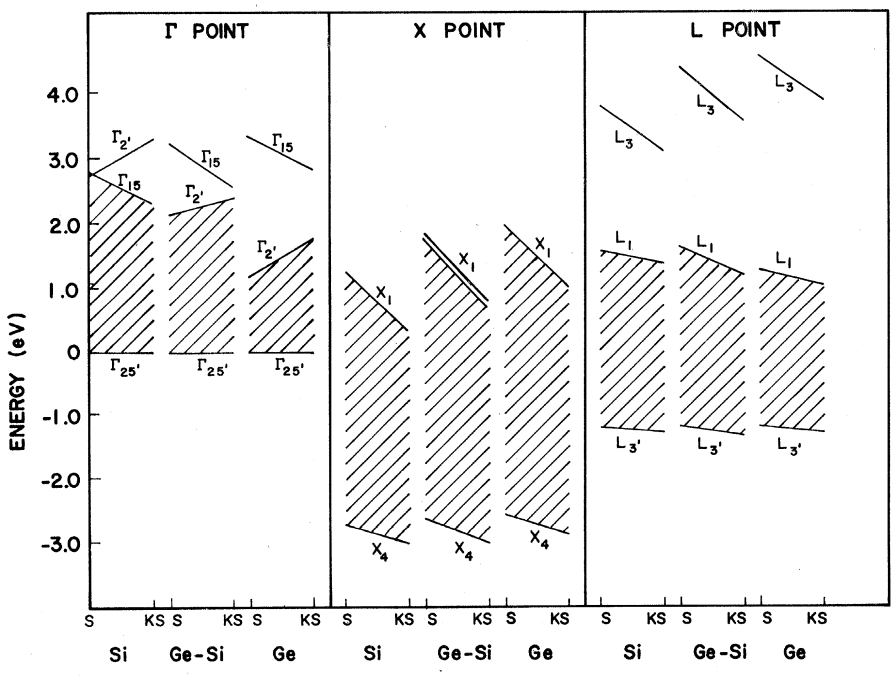

FIG. 2. Variation of the Γ, X, and L high-symmetry-point eigenvalues of Si, Ge-Si, and Ge vs the exchange parameter α. α varies from the Kohn and Sham value to the Slater value. The energies are in eV.

TABLE II. Lattice constants used in the SCOPW band calculations. The lattice constants are given in a.u.

Si	5.431 (Ref. 22)
Ge-Si	5.5373 (Ref. 23)
Ge	5.6575 (Ref. 23)

trons at the Γ, X, L, W, Δ $(\frac{1}{2}, 0, 0)$, and $\Sigma(\frac{1}{2}, \frac{1}{2}, 0)$ high-symmetry points of the Brillouin zone shown in Fig. 1. The weights are taken to be proportional to the volumes within the first Brillouin zone closest to each high-symmetry point. The use of the six-point weighted average has been studied and shown to result in errors of less than 0.1 eV in the energy eigenvalues.[6, 9, 12]

The starting crystal potential is represented by a spatial superposition of nonrelativistic self-consistent atomic potentials in the manner of Herman and Skillman.[13] This crystal-potential model (due to Herman), which is sometimes called the isolated atom or the overlapping free-atom model, also forms the basis of non-self-consistent OPW (NSCOPW) band calculations.

One way of taking relativistic effects into account within the framework of nonrelativistic band calculations is with first-order perturbation theory. The perturbing Hamiltonian obtained for the spin-orbit splitting is

$$\hat{H}_{so} = -\tfrac{1}{4} i q^2 \hat{\sigma} \cdot [\nabla \vec{V}(r) \times \nabla] ,$$

where $V(r)$ is the potential, $\hat{\sigma}$ is the Pauli spin operator, and q is the fine-structure constant. The $\Gamma_{25'}$ SCOPW valence wave functions are used in this calculation.

In order to calculate the density of states and the absorptive part of the dielectric constant ϵ_2, a pseudopotential fit is made to the relevant energy levels at the Γ, X, L, W, Δ, and Σ points. The pseudopotential technique is then used to calculate energy differences and transition-matrix elements throughout the Brillouin zone.[14] In our experience this procedure gives the ϵ_2 peaks at the correct energies. However, the relative peak heights do not match experiment because of their dependence upon the poor pseudopotential wave functions, complicated electron-hole and electron-phonon interactions which are ignored in our model, and neglect of local electric field effects.

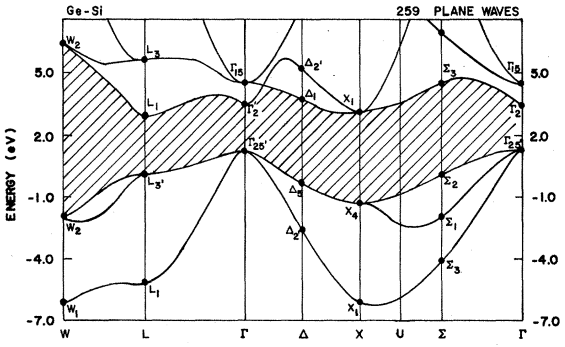

FIG. 4. Self-consistent OPW energy-band structure of Ge-Si obtained using Slater's exchange. The solid dots denote SCOPW energy levels. The solid lines were obtained by fitting a pseudopotential-type interpolation scheme to the SCOPW energy levels.

OPW Series Convergence

In all OPW band calculations it is important to

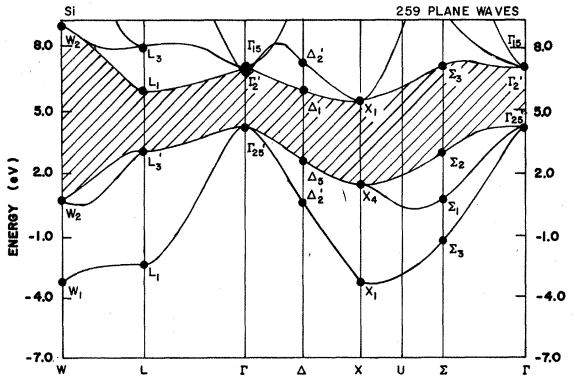

FIG. 3. Self-consistent OPW energy-band structure of Si obtained using Slater's exchange. The solid dots denote SCOPW energy levels. The solid lines were obtained by fitting a pseudopotential-type interpolation scheme to the SCOPW energy levels.

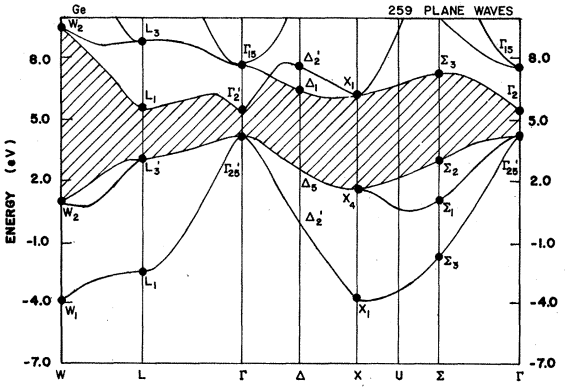

FIG. 5. Self-consistent OPW energy-band structure of Ge obtained using Slater's exchange. The solid dots denote SCOPW energy levels. The solid lines were obtained by fitting a pseudopotential-type interpolation scheme to the SCOPW energy levels.

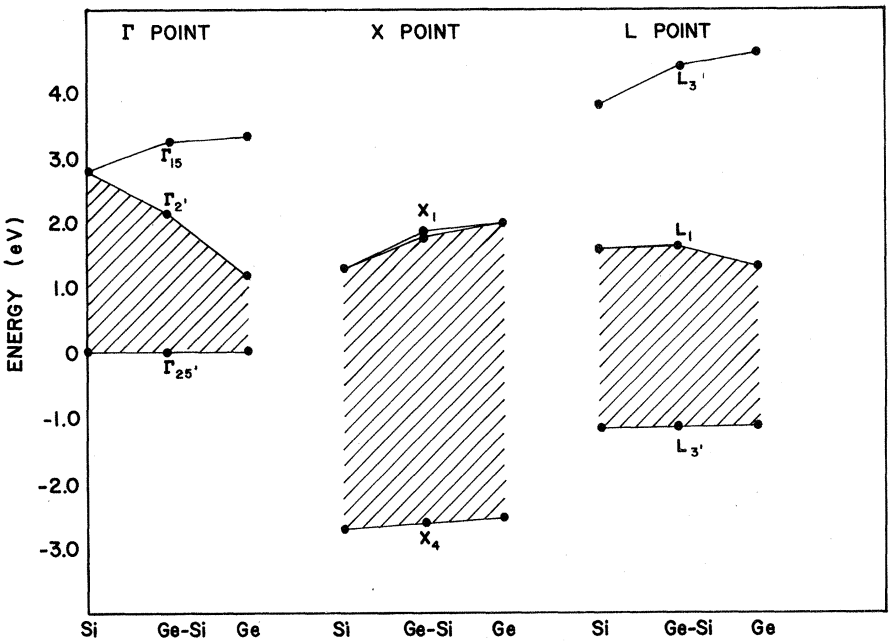

FIG. 6. Variation of the Γ, X, and L high-symmetry-point Slater eigenvalues vs composition. The energies are in eV.

make sure that enough OPW terms are included in the variational wave functions to insure a high degree of convergence. The convergence properties of NSCOPW band calculations for Si, Ge-Si, and Ge are illustrated in Table I. The convergence is very good for all three compounds. The convergence properties of the energy levels at other high-symmetry points in the zone are similar to those shown in Table I. The convergence properties of SCOPW band calculation are very similar to those of the NSCOPW band calculations.[15]

Choice of Exchange Potential

In setting up the SCOPW model one must decide how to handle the exchange and correlation terms. Since no one has been successful in performing a true Hartree-Fock calculation for a crystal one of the local exchange approximations must be used. The three most widely used exchange approximations are due to Slater,[16] Kohn and Sham[17] (also Gaspar[18]), and Liberman.[19] The Slater exchange term is given by

$$V_{xs}(r) = -(6/2\pi)\,k_F(r),$$

where $k_F(r) = [3\pi^2\rho(r)]^{1/3}$ or $[E_F - V(r)]^{1/2}$. The Kohn and Sham exchange term differs by a factor of $\frac{2}{3}$ from Slater's.

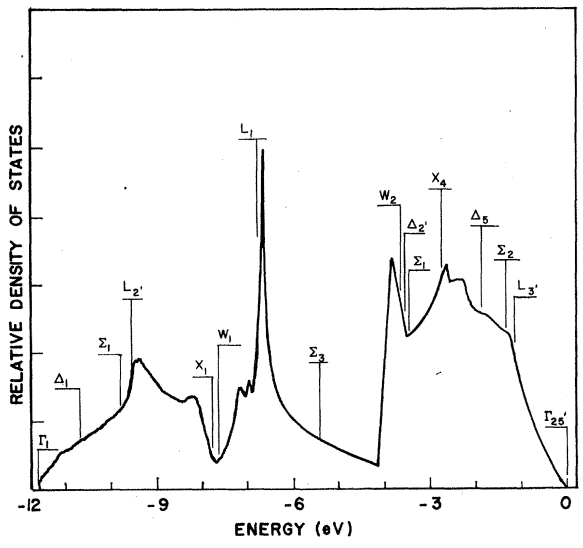

FIG. 7. Electronic density of states for the valence bands of Si.

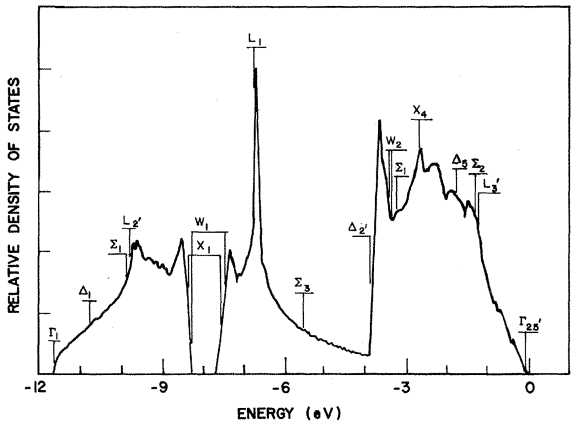

FIG. 8. Electronic density of states for the valence bands of Ge-Si.

TABLE III. Self-consistent energy eigenvalues for Si, Ge-Si, and Ge based on a six-point (Γ, X, L, W, Δ, and Σ) zone sampling and Slater's exchange. 259 OPW's were used at Γ and a comparable number of OPW's at the other high-symmetry points. The lattice constants used were 5.431 Å for Si, 5.5373 Å for Ge-Si, and 5.6575 Å for Ge. The zero of energy has been placed at the top of the valence band ($\Gamma_{25'}$). All entries are in eV.

Level	Si	Ge-Si	Ge
Γ_{15c}	2.79	3.22	3.34
$\Gamma_{2'c}$	2.75	2.14	1.20
$\Gamma_{25'v}$	0.0	0.0	0.0
Γ_{1v}	−11.74	−11.81	−11.88
X_{4c}	9.79	10.10	10.04
X_{1c}	1.28	1.85 1.79	1.97
X_{4v}	− 2.72	− 2.62	− 2.56
X_{1v}	− 7.75	− 7.53 − 8.35	− 8.18
$X_{1c}-X_{4v}$	4.00	4.47 4.41	4.53
L_{3c}	3.83	4.40	4.60
L_{1c}	1.60	1.63	1.30
$L_{3'v}$	− 1.18	− 1.16	− 1.16
L_{1v}	− 6.75	− 6.68	− 6.78
$L_{2'v}$	− 9.53	− 9.77	− 9.93
$L_{3c}-L_{3'v}$	5.01	5.56	5.76
$L_{1c}-L_{3'v}$	2.78	2.79	2.46
W_{1c}	5.15	5.42 5.29	5.60
W_{2c}	4.83	5.56 5.16	5.22
W_{2v}	− 3.57	− 3.29 − 3.38	− 3.18
W_{1v}	− 7.61	− 7.40 − 8.27	− 8.10
$W_{2c}-W_{2v}$	8.40		8.40
$\Delta_{2'c}$	3.62	3.93	3.75
Δ_{1c}	1.55	2.01	2.12
Δ_{5v}	− 1.78	− 1.69	− 1.64
$\Delta_{2'v}$	− 3.58	− 3.80	− 4.16
Δ_{1v}	−10.69	−10.81	−10.92
$\Delta_{1c}-\Delta_{5v}$	3.33	3.70	3.76
Σ_{4c}	5.02	5.45	5.52
Σ_{3c}	2.88	3.17	3.04
Σ_{2v}	− 1.27	− 1.23	− 1.23
Σ_{1v}	− 3.45	− 3.23	− 3.12
Σ_{3v}	− 5.40	− 5.54	− 5.84
Σ_{1v}	− 9.74	− 9.91	−10.06
$\Sigma_{3c}-\Sigma_{2v}$	4.15	4.40	4.27

Our experience on tetrahedrally bonded semiconductors is that Kohn and Sham's exchange gives bands which are too compressed, while those obtained using Liberman's r-dependent state-dependent exchanges are too spread out. The bands obtained using Slater's exchange match experiment very well. Thus Slater's exchange seems to simulate both exchange and correlation for these crystals.[20] The many-body work of Hedin, Lundqvist, and co-workers supports using the $\rho^{1/3}$ approximation to represent exchange-correlation and relaxation effects.[21]

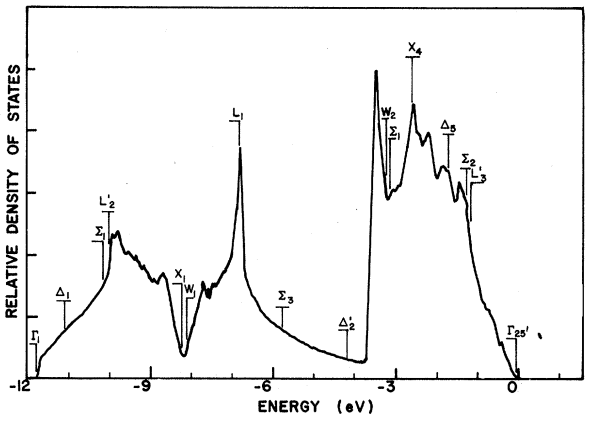

FIG. 9. Electronic density of states for the valence bands of Ge.

Figure 2 shows the effect of going from Slater's exchange to Kohn and Sham's exchange for the three compounds. The sensitivity to the change in exchange coefficient is nearly the same for the three

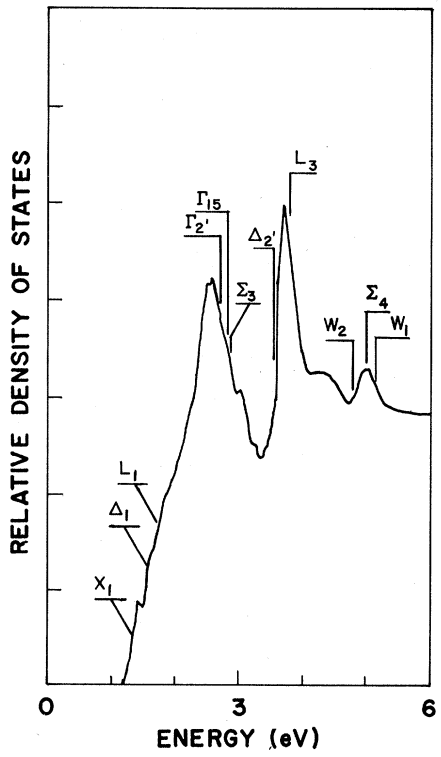

FIG. 10. Electronic density of states for the conduction bands of Si.

TABLE IV. Γ point responsible for changes of direct gap and movement of indirect gap.

	Si		GeSi		Ge	
	SCOPW	Expt	SCOPW	Expt	SCOPW	Expt
Indirect gap	$1.10(\Delta_{1c}^{\min})$	1.13 [a]	$1.61(\Delta_{1c})$	1.1[b], 1.05[c], 0.95[d]	$1.30(L_{1c})$	0.76[e]
Direct gap	$2.75(\Gamma_{2'c})$		$2.14(\Gamma_{2'c})$	~2.24[f]	$1.20(\Gamma_{2'c})$	0.90[e]

[a]Reference 24.
[b]Reference 25.
[c]Reference 26.
[d]Reference 27.
[e]Reference 28.
[f]Reference 29.

compounds. Some levels show remarkably different behavior as the exchange coefficient is varied. For example, the $\Gamma_{2'}$ and Γ_{15} levels move in different directions as the exchange constant is varied.

III. RESULTS

Energy Bands

The SCOPW model contains no adjustable parameters. However, one must put in the lattice constant. The lattice constants used in these calculations are given in Table II.

The energy bands obtained using the six-point sampling technique and Slater's exchange are shown in Figs. 3–5. The eigenvalues are given in Table III. These calculations were made using 259 OPW's at the Γ point and a comparable number of OPW's at the other symmetry points.

The band structure of the three compounds is very similar away from the Γ point. The dissimilarity at the Γ point is due to an increase in the separation of the $\Gamma_{2'c}$ and Γ_{15c} which is 0.04 eV for Si, 1.08 eV for Ge-Si, and 2.14 eV for Ge. This dramatic shift at the Γ point is responsible for the changes of the direct gap and the movement of the indirect gap around the zone (see Table IV). The 0.54 eV difference between the SCOPW and experimental results on the indirect gap of Ge is the largest deviation found on any of the 20 compounds which have been studied using the SCOPW model. This difference could be due to either a model defect or a failure of the Slater-exchange approximation. The experimental data presented for Ge-Si are the results obtained by several workers for the $Ge_{0.5}Si_{0.5}$ alloy. The difference between the SCOPW and experimental results for Ge-Si could stem from the difference between the ideal Ge-Si crystal and the 50% alloy, from a defect in the model, or from the exchange approximation which was used in the model.

Figure 6 shows the variation of the top valence bands and bottom conduction bands from Si to Ge-Si to Ge. The $\Gamma_{25'}$ has been zeroed for all three compounds. The variation is very nearly linear for the top valence bands. Large departures from linearity are found in the conduction bands. Note in particular the Ge-Si X_{1c} which is very close to the Ge X_{1c}, and the Ge-Si L_{1c} which is very close to the Si L_{1c}.

TABLE V. Deformation energies are given for Si, Ge-Si, and Ge. They are based on self-consistent calculations performed at three different lattice constants using Slater's exchange and 259 OPW's. Deformation energies are in eV per unit dilation.

Level	Si	Ge-Si	Ge
Γ_{15c}	14.0	12.8	12.9
$\Gamma_{2'c}$	28.2	23.7	24.0
$\Gamma_{25'v}$	11.8	11.7	11.6
Γ_{1v}	5.3	5.4	5.4
X_{1c}	9.3	10.8 11.3	11.3
X_{4v}	8.9	9.0	8.8
X_{1v}	8.8	8.4 9.3	9.0
L_{3c}	11.9	12.6	13.0
L_{1c}	16.0	16.2	16.2
$L_{3'v}$	10.4	10.6	10.4
W_{2c}	11.9	12.2 16.9	17.3
W_{2v}	7.5	7.8 7.7	7.6
Δ_{1c}	11.0	11.5	10.7
Δ_{5v}	9.6	9.8	9.7
Σ_{3c}	13.5	14.7	15.3
Σ_{2v}	10.3	10.4	10.3

Hydrostatic Pressure

To calculate the effects of hydrostatic pressure

TABLE VI. Theoretical and experimental $\Gamma_{25'v}$ spin-orbit splittings of Si, Ge-Si, and Ge. The theoretical splitting of the $\Gamma_{25'v}$ level (Γ_8-Γ_7) was calculated by first-order perturbation theory using the self-consistent wave functions. All energies are in eV.

	Theoretical	Experimental	
Si	0.056	0.044	(Ref. 33)
Ge-Si	0.207	0.23	(Ref. 34)
Ge	0.338	0.282	(Ref. 35)

TABLE VII. Comparison of theoretical and experimental peak positions for Si, Ge-Si, and Ge.

Si			Ge-Si			Ge		
Theoretical ϵ_2 Present work	Experimental ϵ_2	Reflectivity	Theoretical ϵ_2 Present work	Experimental [a] ϵ_2	Reflectivity	Theoretical ϵ_2 Present work	Experimental [a] ϵ_2	Reflectivity
		3.4[b,c]	3.16	2.9	2.8	2.60	2.2, 2.4	2.2, 2.4
4.10	4.3[d,e]	4.5[d,e]	4.50	4.35	4.5	4.48	4.4	4.6
5.01	5.3[d]	5.7[a]	5.64	5.7	5.9	5.76	5.8	6.1

[a]Reference 36.
[b]Reference 37.
[c]Reference 38.
[d]Reference 39.
[e]Reference 40.

on the band energies we iterated to self-consistency using lattice constants of 5.42 and 5.44 Å for Si, 5.5273 and 5.5473 Å for Ge-Si, and 5.6475 and 5.6675 Å for Ge in addition to the equilibrium lattice constants in Table II. The results are presented in Table V. The deformation energies are defined as

$$E_D = -\frac{\delta E}{\delta V/V} = \frac{\delta E}{3\delta a/a}$$

and are given in units of eV per unit dilation. "a" is the lattice constant.

The valence-band deformation energies are almost identical for all three compounds. The conduction-band deformation energies for the three compounds vary with the values of the Ge-Si deformation energies being generally closer to those of Ge than to those of Si.

For Si the calculated net deformation energy difference for $\Delta_{1c}^{\min} - \Gamma_{25'v}$ is (1.6 ± 0.4) eV per unit dilation where Paul and Brooks measured 1.5 eV per unit dilation[30] and Balslev measured 3.71 eV per unit dilation.[31] For Ge the calculated net deformation energy difference for $L_{1c} - \Gamma_{25'v}$ is (-4.6 ± 0.9) eV per unit dilation, where Paul and Brooks measured -3.8 eV per unit dilation.[30] Cardona and Paul have measured a deformation energy difference of -9.6 ± 0.8 for the $\Gamma_{2'c} - \Gamma_{25'v}$, whereas the calculated value is -12.4 ± 1.0 eV per unit dilation.[32]

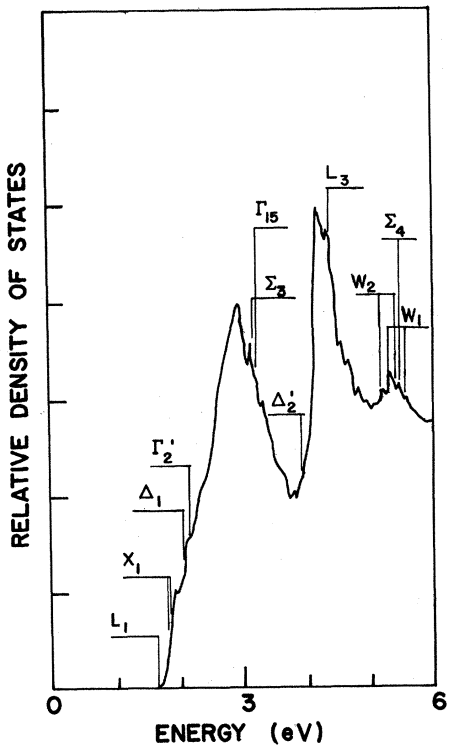

FIG. 11. Electronic density of states for the conduction bands of Ge-Si.

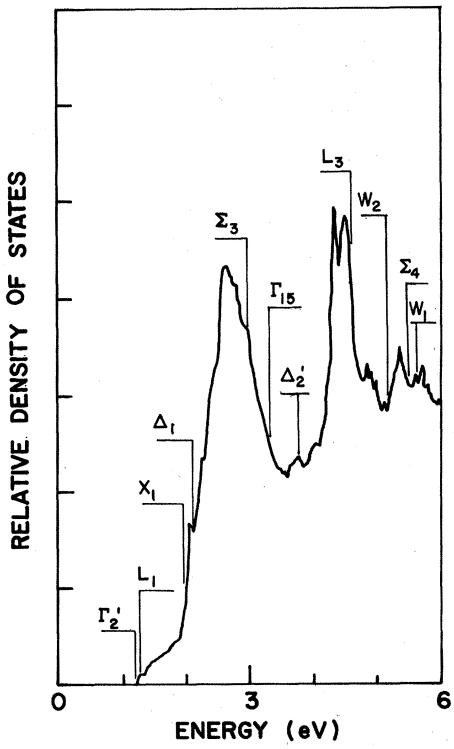

FIG. 12. Electronic density of states for the conduction bands of Ge.

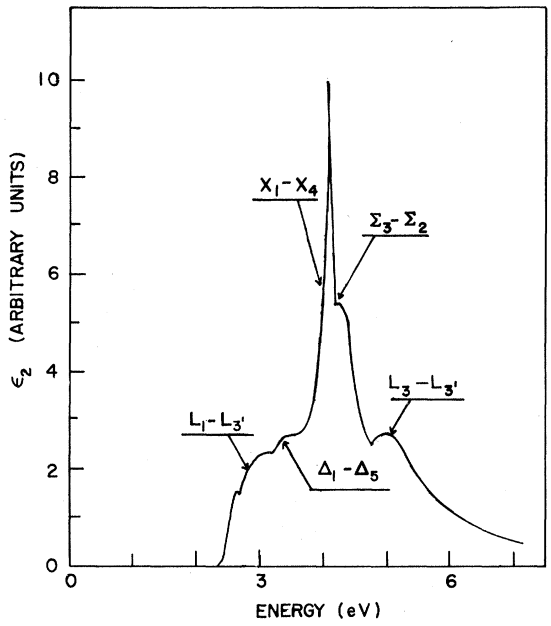

FIG. 13. Theoretical Si ϵ_2 curve derived from the SCOPW energy bands obtained using Slater's exchange.

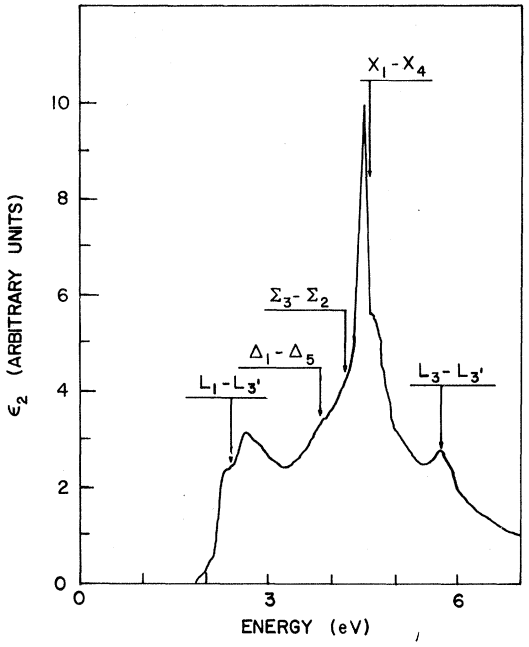

FIG. 15. Theoretical Ge ϵ_2 curve derived from the SCOPW energy bands obtained using Slater's exchange.

Spin-Orbit Splitting

The spin-orbit splitting at the Γ point of the three-fold degenerate $\Gamma_{25'v}$ wave function was found from first-order perturbation theory. The values obtained for Si, Ge-Si, and Ge are shown in Table VI together with the experimental values. For both theoretical and experimental splittings the Ge-Si splitting almost coincides with the value obtained by linear interpolation of the pure-Ge and -Si splittings. Braunstein found a linear variation of the spin-orbit splitting in going from pure Ge to pure Si.[34] Kline *et al.* also performed measurements of the splitting over a limited range of alloys (up to 22.6% Si) but did not find a linear variation.[29]

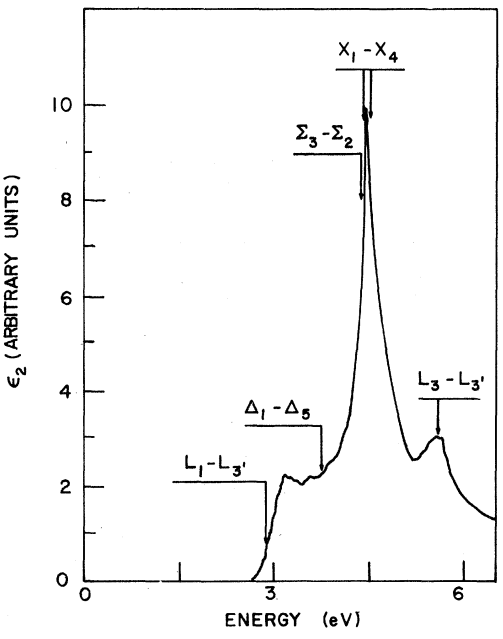

FIG. 14. Theoretical Ge-Si ϵ_2 curve derived from the SCOPW energy bands obtained using Slater's exchange.

Density of States

In Figs. 7–9 the SCOPW density of states for the valence bands is given for the three compounds. The zero of energy for the valence-band density of states was taken at the top of the $\Gamma_{25'v}$ valence band. The location of the high-symmetry-point bands is shown. It should be emphasized that these are merely the locations of high-symmetry-point bands and do not imply that the given structure is due to the particular band.

In the valence-band density of states the first broad peak below the top of the valence band is due to states near L_3', Σ_2, Δ_5, X_4, Σ_1, $\Delta_{2'}$, and W_2. The next peak down originates in the flat area around L_1. The lowest peak is due to the s-like valence band. The valence-band densities of states are very similar for the three compounds. The Ge-Si density of states is slightly more like that of Ge than Si. The $\Delta_{2'}$ level is the only level which moves very much with respect to the structure of the density of states.

TABLE VIII. Experimental and calculated structure factors for Si, Ge-Si, and Ge. RHF values give the results for relativistic Hartree-Fock free atomic charge densities packed in the crystal lattice. S stands for Slater's exchange. KS stands for Kohn-Sham-Gaspar's exchange. Structure factor units are electrons per crystallographic unit cell.

	Si				Ge-Si			Ge			
hkl	Expt[a]	RHF	S	KS	RHF	S	KS	Expt[a]	RHF	S	KS
111	11.12±0.04	10.53	10.88	10.69	116.96	119.04	117.65	27.5±0.12	27.38	27.79	27.53
002	0.00	0.00	0.00	0.00	64.95	65.22	64.63		0.00	0.00	0.00
220	8.78±0.09	8.71	8.77	8.64	129.57	130.32	128.54		23.79	23.94	23.64
311	8.05±0.07	8.16	8.11	8.01	94.54	94.52	93.27		22.36	22.39	22.09
222	0.22±0.04	0.00	0.19	0.17	54.55	55.13	54.20		0.00	0.24	0.21
400	7.40±0.14	7.51	7.54	7.44	111.21	111.81	110.12		20.45	20.60	20.27
313	7.32±0.12	7.18	7.34	7.21	82.25	83.74	82.09		19.49	19.82	19.46
204	0.00	0.00	0.00	0.00	47.07	47.73	46.74		0.00	0.00	0.00
422	6.72±0.06	6.70	6.81	6.68	98.43	99.93	97.91		18.08	18.36	18.00
333	6.43±0.08	6.44	6.51	6.38	73.08	73.99	72.46		17.34	17.61	17.22
511	6.40±0.08	6.44	6.55	6.42	73.08	74.22	72.65		17.34	17.58	17.24
440	6.04±0.15	6.03	6.17	6.02	88.32	89.98	87.90		16.23	16.53	16.16
424	0.0	0.0	0.0	0.0	37.22	37.79	36.99		0.00	0.01	0.01
444	5.00±0.10	4.97	5.12	4.96	73.18	74.73	72.82		13.50	13.76	13.43

[a]Reference 12.

In Figs. 10–12 the SCOPW density of states for the conduction bands is given. The zero of energy for the conduction-band density of states was taken at the top of the $\Gamma_{25'v}$. In the conduction-band density of states the rapid rise to the first peak is due to the flat areas around L_1 and X_1. The second peak results primarily from the flat area around the L_3. There are much greater variations in the density of states for the conduction bands than there were for the valence bands. With the exception of the $\Gamma_{2'}$ the various energy levels remain in the same relative position to the density of states structure for all three compounds.

Imaginary Part of the Dielectric Constant

The imaginary parts of the dielectric constant ϵ_2 calculated from the energy bands obtained using the six-point zone sampling and Slater's exchange are shown in Figs. 13–15. Table VII gives a summary of the theoretical and experimental peak positions. The experimental results given under Ge-Si are those obtained for the $Ge_{0.5}Si_{0.5}$ alloy. The agreement between the theoretical and experimental peak positions is quite good. For example the experimentally determined values of the second peak are 4.3, 4.35, and 4.4 eV for Si, $Ge_{0.5}Si_{0.5}$ alloy, and Ge, respectively. The calculated peak positions are 4.10, 4.50, and 4.48, respectively, for Si, Ge-Si, and Ge. For all three peaks the theoretical peaks for Ge-Si are very close to the experimental peaks determined by Schmidt[36] for $Ge_{0.5}Si_{0.5}$.

Form Factors

Table VIII compares the experimental structure factors,[12] corrected for thermal and anomalous dispersion, with the results of SCOPW calculations for Si and Ge. Table VIII also gives the Ge-Si structure factors. The theoretical procedures differ by the method used to approximate the exchange potential. The columns headed RHF are obtained by placing relativistic Hartree-Fock free atoms in the crystal lattice. Those headed S give results obtained using the Slater $\rho^{1/3}$ approximation, while KS refers to the use of Kohn-Sham and Gaspar exchange. A detailed discussion of the SCOPW and experimental form factors is given in Ref. 12.

IV. CONCLUSIONS

The band structures of Si, Ge-Si, and Ge are quite similar away from the Γ point. The rather large differences in the band structures near the zone center account for the changes in the direct gap and the movement of the indirect gap around the zone. There is a linear variation in the upper valence bands between Si, Ge-Si, and Ge. However there are rather large departures from linearity found in the conduction bands. This is brought out by the deformation energies, the densities of states, and the ϵ_2 curves. Usually the properties of Ge-Si are slightly more like those of Ge than those of Si.

A comparison of the available experimental data for $Ge_{0.5}Si_{0.5}$ with the theoretical results for Ge-Si reveals no unusual discrepancies. The agreement of the experimental $Ge_{0.5}Si_{0.5}$ ϵ_2 peak positions and the theoretical Ge-Si ϵ_2 peak positions is very good. The differences are 0.26, 0.15, and 0.06 eV for the first three peaks, respectively. The 0.26-eV difference occurs on the first peak position which is always the most difficult to reproduce

theoretically. The difference of 0.5 eV in the theoretical indirect gap of Ge-Si and the experimental indirect gap of the $Ge_{0.5}Si_{0.5}$ alloy may be in part due to a difference between the alloy and the pure crystal but probably is due to a defect in the model or in the exchange approximation used in the model.

[1]D. J. Stukel and R. N. Euwema, Phys. Rev. 188, 1193 (1969).
[2]D. J. Stukel and R. N. Euwema, Phys. Rev. 186, 754 (1969).
[3]T. C. Collins, D. J. Stukel, and R. N. Euwema, Phys. Rev. B 1, 724 (1970).
[4]D. J. Stukel, Phys. Rev. B 1, 3458 (1970).
[5]D. J. Stukel, Phys. Rev. B 1, 4791 (1970).
[6]D. J. Stukel, R. N. Euwema, T. C. Collins, F. Herman, and R. L. Kortum, Phys. Rev. 179, 740 (1969).
[7]R. N. Euwema, T. C. Collins, D. G. Shankland, and J. S. DeWitt, Phys. Rev. 162, 710 (1967).
[8]D. J. Stukel, Phys. Rev. B 2, 1852 (1970).
[9]D. J. Stukel and R. N. Euwema, Phys. Rev. B 1, 1635 (1970).
[10]C. Herring, Phys. Rev. 57, 1169 (1940).
[11]R. N. Euwema, D. J. Stukel, and T. C. Collins, *Proceedings of Conference on Computational Methods* (Plenum, New York, 1970).
[12]P. M. Raccah, R. N. Euwema, D. J. Stukel, and T. C. Collins, Phys. Rev. B 1, 756 (1970).
[13]F. Herman and S. Skillman, *Atomic Structure Calculations* (Prentice-Hall, Englewood Cliffs, N. J., 1963).
[14]R. N. Euwema, D. J. Stukel, T. C. Collins, J. S. DeWitt, and D. G. Shankland, Phys. Rev. 178, 1419 (1969).
[15]R. N. Euwema and D. J. Stukel, Phys. Rev. B 1, 4692 (1970).
[16]J. C. Slater, Phys. Rev. 81, 385 (1951).
[17]W. Kohn and L. J. Sham, Phys. Rev. 140, A1133 (1965).
[18]R. Gaspar, Acta. Phys. Acad. Sci. Hung. 3, 263 (1954).
[19]D. A. Liberman, Phys. Rev. 171, 1 (1968).
[20]D. J. Stukel, R. N. Euwema, T. C. Collins, and V. Smith, Phys. Rev. B 1, 779 (1970).
[21]L. Hedin and S. Lundqvist, in *Solid State Physics*, edited by F. Seitz and D. Turnbull (Academic, New York, 1969), Vol. 23.
[22]H. Kiendl, Z. Naturforsch. 22a, 79 (1967).
[23]J. P. Dismukes, L. Ekstrom, and R. J. Paff, J. Phys. Chem. 68, 3021 (1964).
[24]A. Frova and P. Handler, Phys. Rev. Letters 14, 178 (1965).
[25]A. Levitas, C. C. Wang, and B. H. Alexander, Phys. Rev. 95, 846 (1954).
[26]E. R. Johnson and S. M. Christian, Phys. Rev. 95, 560 (1954).
[27]R. Braunstein, A. R. Moore, and F. Herman, Phys. Rev. 109, 695 (1958).
[28]G. G. MacFarlane, T. P. McLean, J. E. Quarrington, and V. Roberts, Proc. Phys. Soc. (London) 71, 863 (1958).
[29]J. S. Kline, F. H. Pollak, and M. Cardona, Helv. Phys. Acta 41, 968 (1968).
[30]W. Paul and H. Brooks, Progr. Semicond. 84, 585 (1963).
[31]I. Balslev, Phys. Rev. 143, 636 (1966).
[32]M. Cardona and W. Paul, J. Phys. Chem. Solids 17, 138 (1960).
[33]S. Zwerdling, K. J. Button, B. Lox, and L. M. Roth, Phys. Rev. Letters 4, 173 (1960).
[34]R. Braunstein, Phys. Rev. 130, 869 (1963).
[35]M. Cardona, K. L. Shaklee, and F. H. Pollak, Phys. Rev. Letters 23, 37 (1966).
[36]E. Schmidt, Phys. Status Solidi 27, 57 (1968).
[37]U. Gerhardt, Phys. Status Solidi 11, 801 (1965).
[38]B. O. Seraphin and W. Bottka, Phys. Rev. Letters 15, 104 (1965); B. O. Seraphin, Phys. Rev. 140, A1716 (1965).
[39]H. R. Phillipp and H. Ehrenreich, Phys. Rev. 129, 1550 (1963).
[40]M. L. Cohen and J. C. Phillips, Phys. Rev. 139, A912 (1965).

PHYSICAL REVIEW B VOLUME 3, NUMBER 10 15 MAY 1971

Perturbation Theory for a Bound Polaron*

Josef Sak
James Franck Institute, The University of Chicago, Chicago, Illinois 60637
(Received 25 January 1971)

The binding energy of a polaron in a Coulomb potential is determined by the second-order perturbation theory to be $E_B^{(2)} = E_B + \alpha\hbar\omega_0(\frac{1}{6}\beta^2 + \frac{1}{24}\beta^4)$, where α is the Fröhlich coupling constant and $\beta^2 = E_B/\hbar\omega_0$. It is supposed that $\alpha \ll 1$ and $\beta \ll 1$. This improves the earlier calculation of Platzman and brings the perturbation theory to agreement with the result reached previously by the application of field-theoretic methods to the problem of a bound polaron.

I. INTRODUCTION

We will calculate, approximately, the energy of the ground state of an electron bound in a Coulomb potential in a weakly polar semiconductor. The problem is described by the following Hamiltonian[1]:

$$\frac{\vec{p}^2}{2m} - \frac{e^2}{\epsilon_s r} + \omega_0 \sum_{\vec{q}} a_{\vec{q}}^\dagger a_{\vec{q}}$$